

Depletion of SMN by RNA interference in HeLa cells induces defects in Cajal body formation

Cyrille Girard, Henry Neel, Edouard Bertrand and Rémy Bordonné*

Institut de Génétique Moléculaire, CNRS UMR5535, IFR 122, 1919 route de Mende, 34000 Montpellier, France

Received April 10, 2006; Accepted April 28, 2006

ABSTRACT

Neuronal degeneration in spinal muscular atrophy (SMA) is caused by reduced expression of the survival of motor neuron (SMN) protein. The SMN protein is ubiquitously expressed and is present both in the cytoplasm and in the nucleus where it localizes in Cajal bodies. The SMN complex plays an essential role for the biogenesis of spliceosomal U-snRNPs. In this article, we have used an RNA interference approach in order to analyse the effects of SMN depletion on snRNP assembly in HeLa cells. Although snRNP profiles are not perturbed in SMN-depleted cells, we found that SMN depletion gives rise to cytoplasmic accumulation of a GFP-SmB reporter protein. We also demonstrate that the SMN protein depletion induces defects in Cajal body formation with coilin being localized in multiple nuclear foci and in nucleolus instead of canonical Cajal bodies. Interestingly, the coilin containing foci do not contain snRNPs but appear to co-localize with U85 scaRNA. Because Cajal bodies represent the location in which snRNPs undergo 2'-O-methylation and pseudouridylation, our results raise the possibility that SMN depletion might give rise to a defect in the snRNA modification process.

INTRODUCTION

Spinal muscular atrophy (SMA) is a common human genetic disease in which degeneration of the motor neurons of the spinal cord results in subsequent muscular atrophy. The SMA disease results from deletions or mutations in the survival of motor neurons (SMN1) gene (1). The SMN protein is ubiquitously expressed in all tissues of metazoan organisms reflecting the fact that it provides a fundamental activity required by all cells. The protein is present both in the cytoplasm and in the nucleus, where it localizes in Cajal bodies both *in vivo* and in cultured cells, although in some cell lines it is also found in separate bodies called gems (gemini of coiled bodies) (2,3). SMN and several associated proteins

called Gemins form a macromolecular complex involved in the biogenesis of various ribonucleoproteins, such as snoRNPs, the spliceosomal U-snRNPs and the telomerase ribonucleoprotein complex (4–6).

In addition to its function in RNP assembly, the SMN protein might also play a role in nucleocytoplasmic, dendritic or axonal transport. Indeed, the SMN protein colocalizes with cytoskeletal proteins in dendrites and axons of spinal cord motoneurons *in vivo* (7–9). Moreover, SMN localizes in motile granules that are located in neurites and growth cones of cultured neurons (10). Taken together, these results suggest that SMN may be actively transported into neuronal processes and could have a motor neuron-specific function.

Concerning the role of the SMN protein in snRNP biogenesis, it has been shown that the SMN complex is required both for the formation of the Sm core complex and the association of this complex to the U1, U2, U4 and U5 snRNAs (11–13). During this process, SMN interacts with the Sm core proteins by binding to the sDMA rich C-terminal domains of SmB, SmD1 and SmD3 (5,14). The sDMAs modifications in the Sm proteins are carried out by the methylosome, a complex containing the PRMT5 methyltransferase, which allows the transfer of modified Sm proteins to the SMN complex and the association of the Sm core complex to the snRNA (5). Moreover, several observations suggest a role for the SMN complex in generating snRNPs that are competent for nuclear import. Indeed, assembly of spliceosomal snRNPs is a stepwise process that follows an ordered pathway [for a review, see (15)]. After transcription by RNA polymerase II, the snRNAs are exported to the cytoplasm where they associate with the Sm proteins. This binding induces hypermethylation of the snRNA 7-methyl cap by a methylase to form methyl-2,2,7-guanosine cap structure, thereby generating an snRNP bipartite nuclear localization signal, composed of the Sm core complex and the snRNA cap structure. It has been shown that SMN associates with snRNP throughout the cytoplasmic phase of this pathway suggesting that SMN might play multiple functions in snRNP assembly and snRNP nuclear import (11,16–19). In order to define more precisely the roles of the SMN complex in the snRNPs assembly pathway, we used an RNA interference approach to generate SMN-depleted HeLa cells. In this report, we show that depletion of SMN affects Sm core

*To whom correspondence should be addressed. Tel: 33 4 67 61 36 47; Fax: 33 4 67 04 02 31; Email: remy.bordonne@igmm.cnrs.fr.

assembly and gives rise to defects in Cajal bodies formation, indicating that snRNP biogenesis is required for the formation of these nuclear structures. Our results point also to a potential link between a defect in the snRNA post-transcriptional modification process and SMA pathogenesis.

MATERIALS AND METHODS

RNA interference, Cell culture and transfection

Design of target-specific siRNA duplexes were performed as described (20) and selected siRNA sequences corresponding to regions 313–331 and 402–420 of the SMN mRNA sequence were generated. Control siRNAs include scrambled siRNA and an siRNA generated against the sequence of the firefly luciferase.

HeLa cells were grown at 37°C in 5% CO₂ and in DMEM containing 10% fetal calf serum. Cells were transfected with the siRNA duplex using Lipofectamine reagent (Invitrogen) according to the manufacturer's protocol. HeLa cell extracts were prepared according to the protocol described previously (21). For preparation of whole cell extracts, HeLa cells from suspension cultures were harvested and lysed for 30 min on ice in HNTG buffer (20 mM HEPES pH 7.9, 150 mM NaCl, 1% Triton, 30% glycerol, 1 mM MgCl₂, 1 mM EDTA, 1 mM PMSF and Proteases inhibitors). After centrifugation at 18 000g (10 min, 4°C), supernatants were used for western analysis or immunoprecipitation experiments.

Immunofluorescence microscopy, western and northern analyses

Immunofluorescence was performed on cells grown on coverslips, washed in PBS and fixed in 4% (wt/vol) paraformaldehyde in PBS at room temperature (RT) followed by permeabilization with 0.1% Triton X100 in PBS for 5 min at RT. Anti-SMN (Transduction Laboratories) were diluted 1/2000 and p80 coilin was detected with polyclonal rabbit anti-coilin antibody (1/400 dilution). Anti-m₃G antibodies (K121) were purchased from Calbiochem and used at 1/1000 dilution for immunofluorescence. Anti-SmB antibodies (ANA125, Cappel) were diluted at 1/100 for IF and 1/500 for western analysis. Incubations were for 1 h at 25°C in PBS containing 2% BSA, and slides were then washed three times for 3 min in PBS. Secondary antibodies were diluted according to manufacturer instructions. Coverslips were mounted on glass slides using mounting medium (Vectashield) and samples were observed using a Leica fluorescence microscope. Images were acquired with a Coolsnap camera (Photometrics) controlled by the software Metamorph (Universal Imaging).

The protein content of the fractions was determined using BCA protein assay kit (Pierce) and equal amounts of proteins from each lysate were analyzed as described previously (22). Detection was carried out by enhanced chemiluminescence (Pierce). Glycerol gradient centrifugation, immunoprecipitation experiments and northern analyses were as described previously (23,24).

Fluorescent *in situ* hybridization

Synthesis and labelling of antisense U85 RNA probe was performed as described (25). HeLa cells were washed twice in

1× PBS and fixed for 20 min at room temperature in 4% paraformaldehyde followed by overnight permeabilization at 4°C in 70% ethanol. Cells were then washed twice in 2× SSC 50% formamide at room temperature and hybridized overnight at 37°C in 40 µl of a mixture containing 10% Dextran sulfate, 2 mM vanadyl-ribonucleoside complex, 0.02% RNase free BSA, 40 µg *Escherichia coli* tRNA, 2 × SSC, 50% formamide, 60 ng of labelled probe. Cells were then washed four times for 30 min in 2× SSC, 50% formamide at 37°C and rehydrated three times 5 min in 1× PBS. Immunofluorescence was performed as described above.

Preparation of nuclear and cytoplasmic extracts

HeLa cells were removed from dishes by trypsinization and washed twice with ice-cold PBS. Cells were resuspended at ~5 × 10⁶/ml in HMKE buffer (20 mM Hepes pH 7.2, 10 mM KCl, 5 mM MgCl₂, 1 mM EDTA and 250 mM sucrose) containing protease inhibitor cocktail (complete EDTA free, Roche), phenylmethylsulfonyl fluoride (PMSF 1 mM) and digitonin (200 µg/ml). Cells were left on ice for 10 min and then centrifuged at 500g for 10 min at 4°C, to separate cytosol from membranes, nuclei, organelles and cytoskeleton. The supernatant (cytosol) was carefully removed, and the pellet was washed in HMKE buffer without digitonin. To perform nuclear protein extraction, the pellet was solubilized in extraction buffer (0.1 M Tris-HCl pH 9, 0.1 M NaCl, 5 mM KCl, 1 mM CaCl₂, 0.5 mM MgCl₂, 0.5% NP-40 and protease inhibitor cocktail) for 20 min on ice. The samples were then centrifuged at 15 000g for 10 min at 4°C and the supernatant (Nuclear fraction) was carefully removed.

RESULTS

Knockdown of SMN expression in HeLa cells by RNA interference

Target-specific siRNA duplexes of 19 nt RNAs with symmetric 2 nt dT 3' overhangs were selected from the SMN open reading frame and transfected, as well as a control siRNA into HeLa cells. To verify correct SMN depletion, cells were harvested, extracts prepared and examined for SMN levels by western blotting. As shown in Figure 1A and as monitored by quantification analysis (Figure 1B), introducing the siRNA duplex targeting region 313–331 of the SMN mRNA gives rise, after 48 or 72 h, to a decrease in SMN protein level of 70–80% compared with the control while levels of GAPDH protein remained unchanged. Similar results were obtained using another siRNA targeting region 402–420 of the SMN mRNA sequence (data not shown) and the decrease of the SMN protein amount is specific to SMN siRNAs since control siRNA against firefly luciferase or a scrambled siRNA have no effects on SMN protein levels (Figure 1A). In order to confirm correct depletion of the SMN protein, cells were subjected to immunofluorescence studies using anti-SMN antibodies. As expected, in control cells, the SMN protein localized diffusely into the cytoplasm and concentrated in Cajal bodies while in SMN-depleted cells, 80–90% of cells no longer showed cytoplasmic or Cajal bodies fluorescence (Figure 1C).

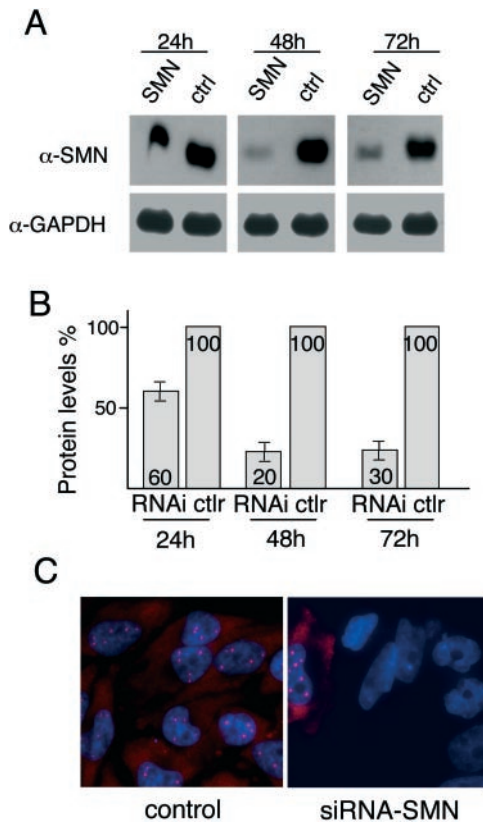


Figure 1. Depletion of SMN in HeLa cells using an RNAi approach (A) western blot analysis on SMN-depleted cells. An siRNA duplex has been transfected into HeLa cells for the indicated time, and extracts were prepared and examined for SMN levels by western blotting using anti-SMN antibodies. A control siRNA was introduced into HeLa cells under similar conditions. The GAPDH protein was used as a loading control. (B) Quantification of SMN protein amounts. Blots were scanned and quantified using ImageQuant software (Molecular Dynamics). The percentage of SMN levels with respect to control is shown. (C) Immunofluorescence studies on SMN-depleted and control HeLa cells using anti-SMN antibodies. In control cells, the SMN protein localizes to the cytoplasm and to Cajal bodies, while cytoplasmic and Cajal bodies fluorescence are no longer visible in the SMN-depleted cells. The nucleus was stained with DAPI. Note that the cell presenting Cajal bodies staining in the SMN-depleted cells (right panel) has not taken up the siRNA and can be considered as a control cell.

Depletion of SMN does not affect the snRNPs profiles on glycerol gradient

In order to test whether SMN depletion might give rise to global defects in the assembly of snRNPs, we examined snRNP complexes in extracts by glycerol gradient sedimentation. Following centrifugation, the RNA of odd-numbered fractions was phenol-extracted and separated on a denaturing polyacrylamide gel. After transfer to a nylon membrane, the blots were then probed with 32 P-labelled oligonucleotides complementary to the spliceosomal snRNAs. As shown in Figure 2, identical snRNP profiles were observed in extracts prepared from both SMN-depleted and control cells: free U6 snRNPs are found in fractions 3–7, the U4/U6 snRNPs sedimented in fractions 9–15 and the multi-U4/U6/U5 snRNPs migrated near the bottom of the gradient in fractions 21–25. U2 and U1 snRNPs were also similarly distributed in both type of cells, being localized in fractions 5–9/13–15 and

5–9 respectively. These results show that snRNPs profiles are not perturbed upon SMN depletion in HeLa cells.

Cytoplasmic retention of a GFP-SmB fusion protein upon SMN depletion

Numerous *in vitro* studies revealed a cytoplasmic role for the SMN protein in the formation of the heptameric Sm core complex and in the association of this complex to the snRNA (5). Accordingly, recent reports showed that knock-down of components of the SMN complex by RNAi inhibited Sm core assembly (26–28). We assumed therefore that depletion of SMN would hinder formation of the Sm core complex in the cytoplasm affecting subsequently the nuclear/cytoplasmic ratio of Sm proteins. Immunofluorescence studies using anti-SmB antibodies did not allow the detection of a significant cytoplasmic accumulation of endogenous SmB (data not shown). In order to visualize a defect in Sm core assembly, we followed the localization of a GFP-SmB fusion protein in the SMN-depleted cells. The GFP-SmB fusion protein was chosen because it does not contain a nuclear localization determinant, in contrast to the SmD1 and SmD3 proteins, indicating that nuclear import and localization into speckles and Cajal bodies is due to incorporation into snRNPs (22,29,30). As shown in Figure 3 and as expected, a speckled distribution and Cajal bodies staining were observed upon transfection of a GFP-SmB plasmid into HeLa cells previously treated with a control siRNA. Interestingly, transfection of the GFP-SmB construct in SMN-depleted cells did not give rise to the clear speckled distribution and Cajal bodies localization of the fusion protein but produced a cytoplasmic accumulation as visualized by an increased fluorescence of this compartment (Figure 3, lower panels). Quantification of these experiments indicated that up to 60–70% of cells show increased cytoplasmic fluorescence in SMN-depleted cells while only 25–35% of cells present this phenotype in control cells. These results demonstrate that cells without SMN display defects in GFP-SmB protein localization, consistent with an inhibition in cytoplasmic Sm core protein assembly.

Depletion of SMN induces defects in Cajal bodies formation

Using anti-coilin antibodies, the immunofluorescence studies shown in Figure 3 also revealed that the SMN-depleted cells display a decreased number and less intense Cajal bodies when compared with control cells. In order to check more precisely this phenotype, we repeated these experiments using both anti-SMN and anti-coilin antibodies. As shown in Figure 4A and as expected, the SMN protein is found in the cytoplasm and colocalizes with coilin in several nucleoplasmic punctuate structures representing canonical Cajal bodies in 70–80% of control HeLa cells (upper panels). In contrast, in SMN-depleted cells (Figure 4A, lower panels), neither cytoplasmic nor nuclear staining was observed using anti-SMN antibodies while small and multiple coilin-positive foci became visible upon anti-coilin staining in 60–70% of cells. The lack of canonical Cajal bodies in SMN-depleted cells is not a consequence of a decrease in the amount of coilin since our western analysis showed that both control and SMN-depleted cells contain equivalent levels of the

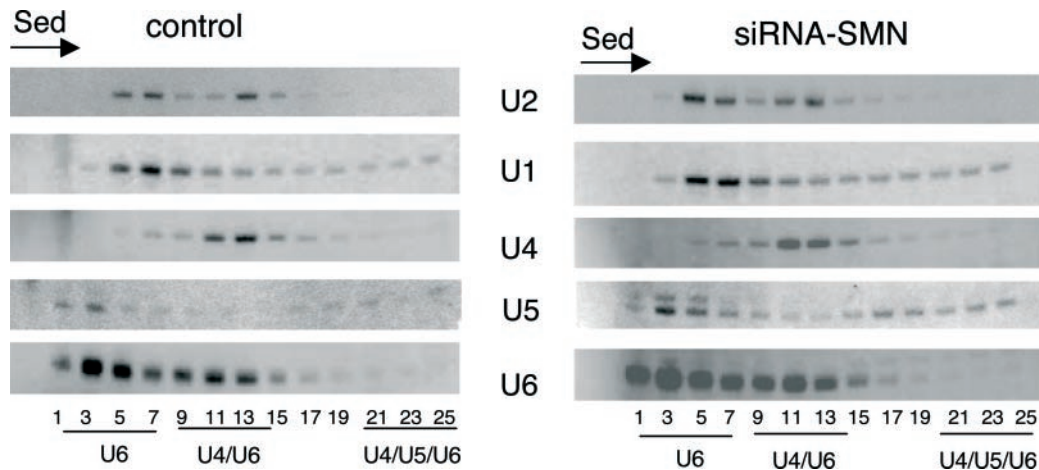


Figure 2. Glycerol gradient sedimentation of snRNPs. Extracts prepared from SMN-depleted (siRNA-SMN) and control cells (control) after 60 h were analyzed by glycerol gradient centrifugation and fractions were recovered. The RNA was extracted, run on denaturing polyacrylamide gels and transferred to a nylon membrane for northern analysis using 32 P-labelled oligonucleotide probes specific for U1, U2, U4, U5 and U6 snRNAs. The fraction number and the positions of the different snRNP complexes are shown at the bottom.

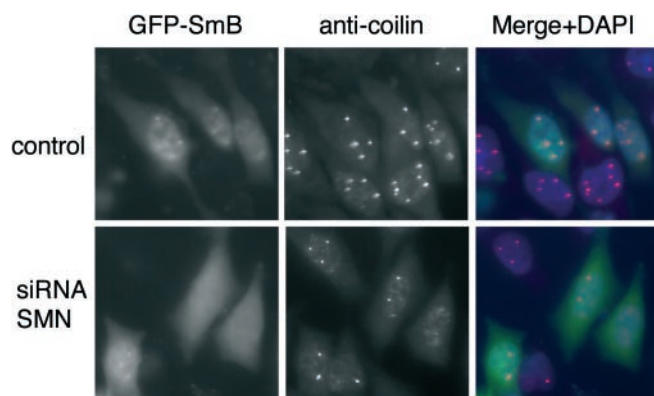


Figure 3. Depletion of SMN hinders the efficient nuclear import of a transiently expressed GFP-SmB fusion protein. After transfection of HeLa cells with a siRNA duplex specific to SMN or a control siRNA for 36 h, cells were transfected with a plasmid encoding a GFP-SmB gene. After 24 h, cells were fixed and the subcellular localization of the GFP-SmB fusion protein was then observed by fluorescence microscopy. Cajal bodies were visualized by immunofluorescence using anti-coilin antibodies. As shown in the upper panels, in control cells, the GFP fusion protein localizes to the nuclear compartment and in Cajal bodies while in the SMN-depleted cells (lower panels), a cytoplasmic accumulation of the GFP-SmB fusion protein is observed.

p80-coilin protein (data not shown). Moreover, examination of the localization of coilin in SMN-depleted cells indicated also a redistribution of coilin protein into the nucleolus. Indeed, as shown in Figure 4B, coilin accumulated only in Cajal bodies in control cells (panels a–d) while in SMN-depleted cells, coilin was dispersed over the nucleoplasm in residual Cajal bodies and could also be found in nucleoli (panels e–h). It appears that coilin accumulated adjacent to the fibrillarin marker of the dense fibrillar region since staining did not cover exactly the same parts of the nucleolus (Figure 4B, panel g). These results demonstrate that the SMN protein is required for correct Cajal body formation and restrained localization of coilin into these structures.

snRNPs do not localize to residual Cajal bodies in SMN-depleted cells

Previous studies indicated that coilin depletion gives rise to residual Cajal bodies unable to recruit snRNPs and the SMN complex (31–33). To determine whether the residual Cajal bodies observed in SMN-depleted cells contained spliceosomal snRNPs, we stained both control and SMN-depleted cells with anti-coilin antibodies and with anti- m_3G antibodies, the latter recognizing the m_3G cap of mature snRNAs. As shown in Figure 5, in control HeLa cells, the m_3G cap epitope colocalized with coilin into the canonical Cajal bodies confirming that snRNPs are found in these structures (29,34). In addition, a diffuse nucleoplasmic m_3G staining was also observed and corresponded to localization of snRNPs in speckles that are compartments enriched of pre-messenger RNA splicing factors (35). In SMN-depleted cells, residual Cajal bodies are visualized by coilin immunofluorescence while anti- m_3G antibodies staining produced a diffuse nucleoplasmic and nuclear speckled distribution suggesting that snRNPs are located in speckles (Figure 5, lower panels). However, this m_3G staining did not co-localize with the positive-coilin foci indicating that upon SMN depletion, the residual Cajal bodies do not contain snRNPs.

The U85 scaRNA is located in residual Cajal bodies

Previous studies demonstrated that Cajal bodies contain small Cajal body-specific RNAs (scaRNAs) that function in the post-transcriptional modification of polII-specific spliceosomal snRNAs (25,36,37). Because it appears that snRNPs do not colocalize with residual Cajal bodies in SMN-depleted cells, we investigated the intracellular localization of the U85 scaRNA upon SMN depletion. Owing to the low amount of endogenous U85 scaRNAs, cells were co-transfected with a plasmid encoding the U85 gene (25) together with the siRNA duplex and used in *in situ* experiments after 48 h growth. As shown in Figure 6 (upper panels), probing of control HeLa cells using a fluorescent

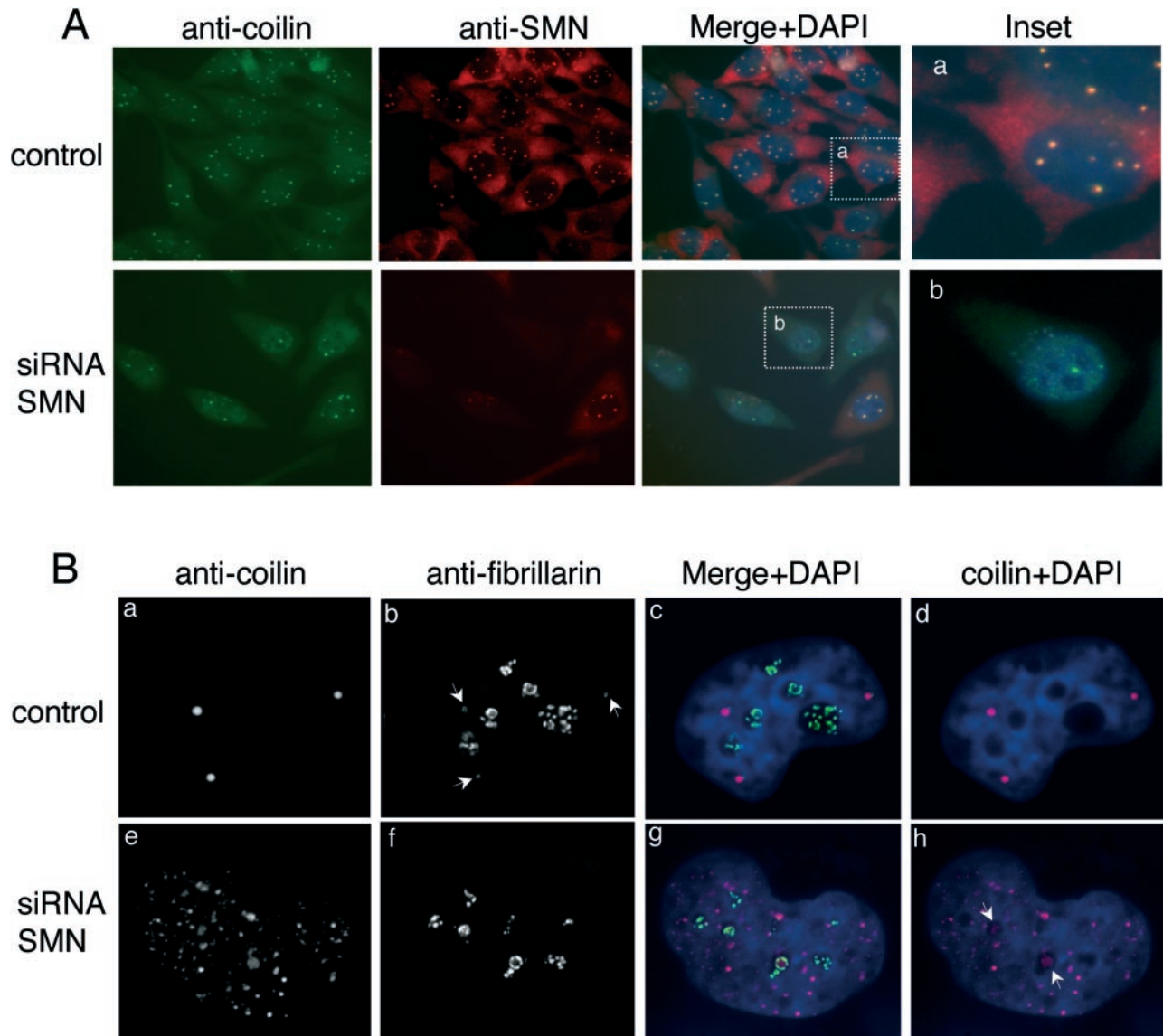


Figure 4. SMN-depleted cells contain numerous foci reacting with coilin antibodies. (A) Immunofluorescence studies with antibodies directed against coilin and SMN were performed on control cells and on SMN-depleted cells. In control cells, coilin and SMN localizes to canonical Cajal bodies while these structures become dispersed in SMN-depleted cells where coilin localizes to numerous nucleoplasmic foci. Zooms of representative cells corresponding to the insets are represented at the right. (B) Relocalization of coilin into nucleoli upon SMN depletion. Immunofluorescence studies with coilin allows the detection of Cajal bodies in control cells while fibrillarlin is found primarily in nucleoli and also in Cajal bodies (white arrows, panel b). In SMN-depleted cells (lower panels), coilin is found in residual Cajal bodies and in nucleoli (white arrows, panel h) which are stained by fibrillarlin (panels f–g). The nucleus was stained with DAPI.

antisense probe specific for the U85 scaRNA resulted in strong stained dots in the nucleoplasm and these dots also reacted with anti-p80 coilin antibodies showing that they correspond to canonical Cajal bodies. In SMN-depleted cells, the p80-coilin antibodies allowed the staining of multiple small and faint foci corresponding to the residual Cajal bodies and interestingly, these dots were also visible with the U85 antisense probe (Figure 6, lower panels), suggesting that the U85 scaRNA accumulates with the residual Cajal bodies.

DISCUSSION

The SMN protein plays essential roles in the production of spliceosomal snRNPs during the cytoplasmic stages of this

pathway (4,5). The SMN protein also localizes in the nucleoplasm in structures called Cajal bodies, which are important for the maturation of RNPs (38). Previous *in vitro* studies with extracts of SMN-depleted cells confirmed that SMN is required for efficient Sm core assembly (26–28). In this study, we report that a lower Sm assembly activity is also obtained *in vivo* upon SMN depletion. Indeed, while we failed to detect a strong defect in the nuclear import of endogenous Sm proteins, we found that a transiently transfected GFP-SmB fusion protein does not localize clearly in speckles and Cajal bodies and accumulates in the cytoplasm in SMN-depleted but not in control cells. This effect is not because of a difference in the amount of GFP-SmB fusion protein expressed in both type of cells since similar levels are present

as confirmed by Western analysis (data not shown). It is thus conceivable that the visualization of cytoplasmic GFP-SmB upon SMN depletion results from the saturation of the Sm core/snRNP assembly machine due to limiting amount of SMN, the saturation threshold being not reachable in control cells with normal SMN levels.

In addition to its role in Sm core assembly, it has been proposed that the SMN protein plays a role in the snRNP nuclear import process. Indeed, using a digitonin-permeabilized *in vitro* cell system, it was shown that import of labeled U1 snRNPs is dependent on SMN indicating that SMN and snRNP nuclear imports are coupled *in vitro* (18). The fact that we could not detect cytoplasmic snRNP accumulation in SMN-depleted HeLa cells in our RNAi experiments could be due to the rapid degradation of the snRNA that is unable to associate to a complete Sm core complex. An instability of the non-assembled snRNA is consistent with studies in yeast showing that depletion of a unique Sm protein inhibits Sm core assembly and leads to degradation of U-snRNAs (39). It is also possible that, *in vivo*, snRNPs are imported into the nucleus by multiple pathways. The existence of various import routes for snRNPs can be compared

with the import pathways of ribosomal proteins whose nuclear localization signals are represented by an accumulation of basic aminoacids and which can be imported by four different transporters (40). It is noteworthy that the nuclear localization signal of the snRNP common core proteins is represented by a basic rich protuberance (22), which could be recognized by other nuclear import receptors in the absence of SMN.

Our inability to detect clear *in vivo* loss-of function defects in snRNP assembly in SMN-depleted cells could also be due to the fact that snRNPs are very stable and have long half-life of >60 h (41). It is therefore conceivable that snRNPs are recycled many times, hindering analysis of effects on newly synthesized snRNPs. Alternatively, it is also possible that depletion of SMN gives rise to more subtle defects in the Sm core complex and snRNP assembly processes and that these defects do not generate snRNP instability or snRNP cytoplasmic accumulation. Although purified Sm proteins assemble on snRNAs in an ordered pathway *in vitro* (42), the SMN machinery could play a role in controlling the specificity and stoichiometry of Sm proteins in the heptameric ring complex. Depletion of the SMN protein could therefore lead to a defect in a 'quality control' process, which would generate abnormal heptameric Sm core complexes that would not obligatorily be hindered in their association to snRNAs. Such a defect could subsequently generate several types of aberrant snRNPs, being defective at different steps in the snRNP biogenesis pathway. For example, an aberrant Sm core complex lacking the SmE protein would still be able to associate with an snRNA, be substrate for the Tgs1 hypermethylase (recognizing the C-tails of SmB and SmD1 proteins) and the resulting snRNPs able to be imported in the nucleus and to localize into Cajal bodies and speckles. Similarly, a snRNP lacking SmB would still be recognized by the Tgs1 enzyme (owing to the interaction of the enzyme with SmD1) and also be competent for nuclear import. However, these aberrant snRNPs could be partially deleterious in steps affecting spliceosome assembly and/or pre-mRNA splicing. The formation of multiple abnormal snRNPs, being still able to follow a correct snRNP biogenesis pathway, could explain the difficulties to see prominent loss-of-functions defects in snRNP formation and subcellular localization in SMN-depleted cells.

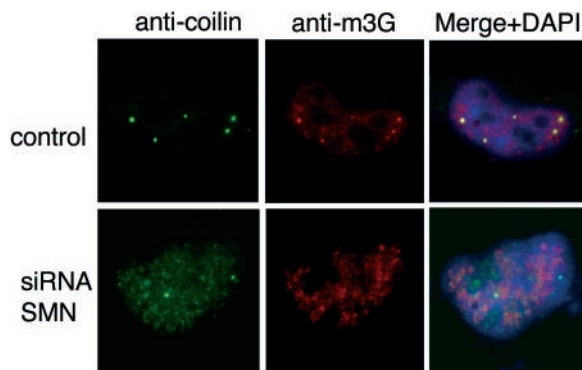


Figure 5. snRNPs do not localize in residual Cajal bodies observed in SMN-depleted cells. To determine the localization of snRNPs, control cells and SMN-depleted cells were subjected to immunofluorescence studies using anti-p80 coilin (red) and anti-m₃G antibodies (green). In control cells, snRNPs accumulate into Cajal bodies and into speckles while in SMN-depleted cells, snRNPs are not located into residual Cajal bodies but are found in a diffuse speckled distribution.

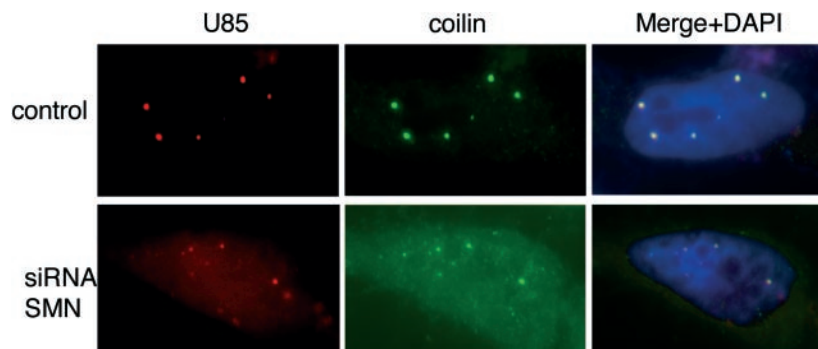


Figure 6. *In situ* localization of U85 scaRNA. A plasmid containing human U85 scaRNA was transfected into HeLa cells with control or SMN specific siRNA duplexes and after 48 h, cells were subjected to *in situ* hybridization using a Cy3-fluorescent probe specific to U85 (red). The canonical Cajal bodies in control cells and the residual Cajal bodies in SMN-depleted cells were visualized with anti-p80 coilin antibody staining (green).

By examining SMN-depleted cells using immunofluorescence techniques, we could detect that canonical Cajal bodies visible in wild-type cells were replaced by numerous nuclear coilin-positive foci. Consistent with our data, a recent study report that reduction in the levels of proteins from the SMN complex affects Cajal bodies homeostasis (27). These results suggest that the SMN protein is required for correct Cajal bodies formation and extend to SMN the previous observations that coilin has a crucial role in defining Cajal body structure. Indeed, characterization of coilin knockout MEF cells revealed that residual Cajal bodies are formed in the absence of full-length coilin protein (32). These structures do not contain spliceosomal snRNPs and the SMN protein, but accumulate fibrillar and Nopp140, two nucleolar markers as well as the U3 snoRNA (32,37). Moreover, separate coilin-positive Cajal bodies without SMN and SMN positive foci lacking coilin have been observed in DFSF1 cells after injection of fluorescent tagged coilin or SMN proteins (30). A second type of residual Cajal body accumulating scaRNAs and Sm snRNAs but not the other nucleolar markers has also been found in coilin knockout MEF cells (37). Our findings that SMN depletion affects Cajal bodies formation in HeLa cells are also consistent with other studies showing that reduction in expression of the SMN complex is associated with a failure in the assembly of nuclear bodies. Indeed, immunocytochemical analysis of fibroblasts from type I SMA patients indicates a significant reduction in the number of gems and a correlation of the number of gems with clinical severity (43). In addition, immunofluorescence microscopy experiments on spinal cord of SMA fetuses show that nucleus from cells no longer present SMN-containing foci although Cajal body staining was detectable using fibrillar antibodies (44). Moreover, by homozygous deletion of the SMN exon 7 in neurons of mice affected with an SMA phenotype, it was shown that the mutated SMN protein has a defect in nuclear targeting leading to a defect in formation of nuclear bodies (45). Altogether, these data indicate that SMN plays a critical role in the production and composition of Cajal bodies.

Based on the fact that SMN knock-down leads to formation of residual Cajal bodies containing the U85 scaRNA but not snRNPs, it is tempting to propose that the modification process of internal residues in snRNAs might be defective in SMN-depleted cells. Indeed, it was shown that Cajal bodies are the subnuclear structures in which scaRNAs perform 2'-O-methylation and pseudouridylation at internal residues of spliceosomal snRNAs (36,37,46). It was also shown that several 2'-O-methylated and pseudouridylated residues in U2 snRNA are important for spliceosome formation and for efficient splicing (47). It is therefore conceivable that a defect in the modification process of snRNA internal residues could result in nuanced splicing perturbations of particular pre-mRNAs and to inefficient and/or incorrect production of specific proteins in motoneurons of SMA patients. Such a model could also explain why SMN mutations affect specifically motoneurons. Given that snRNPs are very stable (see above), our preliminary experiments could not allow us to determine whether this process is affected in HeLa cells upon SMN depletion and other studies are clearly needed to address this question. In this

regard, the biochemical defects responsible for the SMA disease are not well understood, and a long unanswered question was to know whether SMA pathogenesis is linked to SMN defects in snRNP biogenesis. A response has recently been provided by an elegant study showing that reduction of SMN levels impairs snRNP assembly and causes motor axon degeneration in zebrafish embryos (28). Remarkably, a compensation of motor axon defects in the embryos is observed upon injection of purified human or *Xenopus* U snRNPs demonstrating a link between motor axon degeneration and snRNP assembly defects. The use of this experimental system with snRNPs reconstituted using *in vitro* transcribed snRNAs and thus lacking modified residues will clearly be helpful to characterize a correlation between a defect in the production of modified residues in snRNAs and motor axon degeneration.

ACKNOWLEDGEMENTS

The authors thank A. Lamond for gifting anti-coilin antibodies and E. Basyuck and F. Rage for critical reading of the manuscript. C.G. was a recipient of a fellowship from the Association Française contre les Myopathies (AFM). This work was supported by the Ligue Nationale contre le Cancer (Equipe Labellisée 2004) and the Centre National de la Recherche Scientifique (CNRS). Funding to pay the Open Access publication charges for this article was provided by the Ligue Nationale contre le Cancer.

Conflict of interest statement. None declared.

REFERENCES

1. Frugier,T., Nicole,S., Cifuentes-Diaz,C. and Melki,J. (2002) The molecular bases of spinal muscular atrophy. *Curr. Opin. Genet. Dev.*, **12**, 294–298.
2. Liu,Q. and Dreyfuss,G. (1996) A novel nuclear structure containing the survival of motor neurons protein. *EMBO J.*, **15**, 3555–3565.
3. Matera,A.G. and Frey,M.R. (1998) Coiled bodies and gems: Janus or gemini? *Am. J. Hum. Genet.*, **63**, 317–321.
4. Paushkin,S., Gubitza,A.K., Massenet,S. and Dreyfuss,G. (2002) The SMN complex, an assemblysome of ribonucleoproteins. *Curr. Opin. Cell Biol.*, **14**, 305–312.
5. Meister,G., Eggert,C. and Fischer,U. (2002) SMN-mediated assembly of RNPs: a complex story. *Trends Cell Biol.*, **12**, 472–478.
6. Bachand,F., Boisvert,F.M., Cote,J., Richard,S. and Autexier,C. (2002) The product of the survival of motor neuron (SMN) gene is a human telomerase-associated protein. *Mol. Biol. Cell.*, **13**, 3192–3202.
7. Bechade,C., Rostaing,P., Cisterni,C., Kalisch,R., La Bella,V., Pettmann,B. and Triller,A. (1999) Subcellular distribution of survival motor neuron (SMN) protein: possible involvement in nucleocytoplasmic and dendritic transport. *Eur. J. Neurosci.*, **11**, 293–304.
8. Pagliardini,S., Giavazzi,A., Setola,V., Lizier,C., Di Luca,M., DeBiasi,S. and Battaglia,G. (2000) Subcellular localization and axonal transport of the survival motor neuron (SMN) protein in the developing rat spinal cord. *Hum. Mol. Genet.*, **9**, 47–56.
9. Cifuentes-Diaz,C., Nicole,S., Velasco,M.E., Borra-Cebrian,C., Panozzo,C., Frugier,T., Millet,G., Roblot,N., Joshi,V. and Melki,J. (2002) Neurofilament accumulation at the motor endplate and lack of axonal sprouting in a spinal muscular atrophy mouse model. *Hum. Mol. Genet.*, **11**, 1439–1447.
10. Zhang,H.L., Pan,F., Hong,D., Shenoy,S.M., Singer,R.H. and Bassell,G.J. (2003) Active transport of the survival motor neuron

- protein and the role of exon-7 in cytoplasmic localization. *J. Neurosci.*, **23**, 6627–6637.
11. Fischer, U., Liu, Q. and Dreyfuss, G. (1997) The SMN-SIP1 complex has an essential role in spliceosomal snRNP biogenesis. *Cell*, **90**, 1023–1029.
 12. Meister, G., Buhler, D., Pillai, R., Lottspeich, F. and Fischer, U. (2001) A multiprotein complex mediates the ATP-dependent assembly of spliceosomal U snRNPs. *Nat. Cell Biol.*, **3**, 945–949.
 13. Pellizzoni, L., Yong, J. and Dreyfuss, G. (2002) Essential role for the SMN complex in the specificity of snRNP assembly. *Science*, **298**, 1775–1779.
 14. Friesen, W.J., Massenet, S., Paushkin, S., Wyce, A. and Dreyfuss, G. (2001) SMN, the product of the spinal muscular atrophy gene, binds preferentially to dimethylarginine-containing protein targets. *Mol. Cell*, **7**, 1111–1117.
 15. Will, C.L. and Lührmann, R. (2001) Spliceosomal UsnRNP biogenesis, structure and function. *Curr. Opin. Cell Biol.*, **13**, 290–301.
 16. Massenet, S., Pellizzoni, L., Paushkin, S., Mattaj, J.W. and Dreyfuss, G. (2002) The SMN complex is associated with snRNPs throughout their cytoplasmic assembly pathway. *Mol. Cell Biol.*, **22**, 6533–6541.
 17. Narayanan, U., Ospina, J.K., Frey, M.R., Hebert, M.D. and Matera, A.G. (2002) SMN, the spinal muscular atrophy protein, forms a pre-import snRNP complex with snurportin1 and importin beta. *Hum. Mol. Genet.*, **11**, 1785–1795.
 18. Narayanan, U., Achsel, T., Lührmann, R. and Matera, A.G. (2004) Coupled *in vitro* import of U snRNPs and SMN, the spinal muscular atrophy protein. *Mol. Cell*, **16**, 223–234.
 19. Mouaiikel, J., Narayanan, U., Verheggen, C., Matera, A.G., Bertrand, E., Tazi, J. and Bordonné, R. (2003) Interaction between the small-nuclear-RNA cap hypermethylase and the spinal muscular atrophy protein, survival of motor neuron. *EMBO Rep.*, **4**, 616–622.
 20. Elbashir, S.M., Harborth, J., Weber, K. and Tuschl, T. (2002) Analysis of gene function in somatic mammalian cells using small interfering RNAs. *Methods*, **26**, 199–213.
 21. Dignam, J.D., Lebovitz, R.M. and Roeder, R.G. (1983) Accurate transcription initiation by RNA polymerase II in a soluble extract from isolated mammalian nuclei. *Nucleic Acids Res.*, **11**, 1475–1489.
 22. Girard, C., Mouaiikel, J., Neel, H., Bertrand, E. and Bordonné, R. (2004) Nuclear localization properties of a conserved protuberance in the Sm core complex. *Exp. Cell Res.*, **299**, 199–208.
 23. Bordonné, R., Banroques, J., Abelson, J. and Guthrie, C. (1990) Domains of yeast U4 spliceosomal RNA required for PRP4 protein binding, snRNP-snRNP interactions, and pre-mRNA splicing *in vivo*. *Genes Dev.*, **4**, 1185–1196.
 24. Camasses, A., Bragado-Nilsson, E., Martin, R., Séraphin, B. and Bordonné, R. (1998) Interactions within the yeast Sm core complex: from proteins to amino acids. *Mol. Cell Biol.*, **18**, 1956–1966.
 25. Darzacq, X., Jady, B.E., Verheggen, C., Kiss, A.M., Bertrand, E. and Kiss, T. (2002) Cajal body-specific small nuclear RNAs: a novel class of 2'-O-methylation and pseudouridylation guide RNAs. *EMBO J.*, **21**, 2746–2756.
 26. Feng, W., Gubitz, A.K., Wan, L., Battle, D.J., Dostie, J., Golembe, T.J. and Dreyfuss, G. (2005) Gemins modulate the expression and activity of the SMN complex. *Hum. Mol. Genet.*, **14**, 1605–1611.
 27. Shpargel, K.B. and Matera, A.G. (2005) Gemin proteins are required for efficient assembly of Sm-class ribonucleoproteins. *Proc. Natl Acad. Sci. USA*, **102**, 17372–17377.
 28. Winkler, C., Eggert, C., Gradl, D., Meister, G., Giegerich, M., Wedlich, D., Lagerbauer, B. and Fischer, U. (2005) Reduced U snRNP assembly causes motor axon degeneration in an animal model for spinal muscular atrophy. *Genes Dev.*, **19**, 2320–2330.
 29. Sleeman, J.E. and Lamond, A.I. (1999) Newly assembled snRNPs associate with coiled bodies before speckles, suggesting a nuclear snRNP maturation pathway. *Curr. Biol.*, **19**, 1065–1074.
 30. Sleeman, J.E., Ajuh, P. and Lamond, A.I. (2001) snRNP protein expression enhances the formation of Cajal bodies containing p80-coilin and SMN. *J. Cell Sci.*, **114**, 4407–4419.
 31. Bauer, D.W. and Gall, J.G. (1997) Coiled bodies without coilin. *Mol. Biol. Cell.*, **8**, 73–82.
 32. Tucker, K.E., Berciano, M.T., Jacobs, E.Y., LePage, D.F., Shpargel, K.B., Rossire, J.J., Chan, E.K., Lafarga, M., Conlon, R.A. and Matera, A.G. (2001) Residual Cajal bodies in coilin knockout mice fail to recruit Sm snRNPs and SMN, the spinal muscular atrophy gene product. *J. Cell Biol.*, **154**, 293–307.
 33. Hebert, H., Shpargel, K.B., Ospina, J.K., Tucker, K.E. and Matera, A.G. (2002) Coilin methylation regulates nuclear body formation. *Dev. Cell*, **3**, 329–337.
 34. Carvalho, T., Almeida, F., Calapez, A., Lafarga, M., Berciano, M.T. and Carmo-Fonseca, M. (1999) The spinal muscular atrophy disease gene product, SMN: a link between snRNP biogenesis and the Cajal (coiled) body. *J. Cell Biol.*, **147**, 715–728.
 35. Spector, D.L., Fu, X.D. and Maniatis, T. (1991) Associations between distinct pre-mRNA splicing components and the cell nucleus. *EMBO J.*, **10**, 3467–3481.
 36. Kiss, A.M., Jady, B.E., Darzacq, X., Verheggen, C., Bertrand, E. and Kiss, T. (2002) A Cajal body-specific pseudouridylation guide RNA is composed of two box H/ACA snoRNA-like domains. *Nucleic Acids Res.*, **30**, 4643–4649.
 37. Jady, B.E., Darzacq, X., Tucker, K.E., Matera, A.G., Bertrand, E. and Kiss, T. (2003) Modification of Sm small nuclear RNAs occurs in the nucleoplasmic Cajal body following import from the cytoplasm. *EMBO J.*, **22**, 1878–1888.
 38. Gall, J.G. (2003) The centennial of the Cajal body. *Nat. Rev. Mol. Cell Biol.*, **4**, 975–980.
 39. Bordonné, R. and Tarassov, I. (1996) The yeast SME1 gene encodes the homologue of the human E core protein. *Gene*, **176**, 111–117.
 40. Jäkel, S. and Görlich, D. (1998) Importin beta, transportin, RanBP5 and RanBP7 mediate nuclear import of ribosomal proteins in mammalian cells. *EMBO J.*, **17**, 4491–5402.
 41. Fury, M.G. and Zieve, G.W. (1996) U6 snRNA maturation and stability. *Exp. Cell Res.*, **228**, 160–163.
 42. Raker, V.A., Plessel, G. and Lührmann, R. (1996) The snRNP core assembly pathway: identification of stable core protein heteromeric complexes and an snRNP subcore particle *in vitro*. *EMBO J.*, **15**, 2256–2269.
 43. Coover, D.D., Le, T.T., McAndrew, P.E., Strasswimmer, J., Crawford, T.O., Mendell, J.R., Coulson, S.E., Androphy, E.J., Prior, T.W. and Burghes, A.H. (1997) The survival motor neuron protein in spinal muscular atrophy. *Hum. Mol. Genet.*, **6**, 1205–1214.
 44. Lefebvre, S., Burlet, P., Liu, Q., Bertrand, S., Clermont, O., Munnich, A., Dreyfuss, G. and Melki, J. (1997) Correlation between severity and SMN protein level in spinal muscular atrophy. *Nat. Genet.*, **16**, 265–269.
 45. Frugier, T., Tiziano, F.D., Cifuentes-Diaz, C., Miniou, P., Roblot, N., Dierich, A., Le Meur, M. and Melki, J. (2000) Nuclear targeting defect of SMN lacking the C-terminus in a mouse model of spinal muscular atrophy. *Hum. Mol. Genet.*, **9**, 849–858.
 46. Jady, B.E. and Kiss, T. (2001) A small nucleolar guide RNA functions both in 2'-O-ribose methylation and pseudouridylation of the U5 spliceosomal RNA. *EMBO J.*, **20**, 541–551.
 47. Donmez, G., Hartmuth, K. and Lührmann, R. (2004) Modified nucleotides at the 5' end of human U2 snRNA are required for spliceosomal E-complex formation. *RNA*, **10**, 1925–1933.